EUROPEAN ORGANIZATION FOR NUCLEAR RESEARCH

BNL 18038

Conf-730531--7

RECENT PROGRESS IN TRANSITION RADIATION DETECTOR TECHNIQUES

Luke C.L. Yuan*)

Brookhaven National Laboratory, Upton, USA

Presented at the
Int. Conf. on Instrumentation for High-Energy Physics
Frascati, 8-12 May 1973

*) Visitor at CERN

RECENT PROGRESS IN TRANSITION RADIATION DETECTOR TECHNIQUES*)

Luke C.L. Yuan**)

Brookhaven National Laboratory,
Upton, N.Y., USA.

A brief review of the principal characteristics of transition radiation is given and a list of some of the major experimental achievements involving charged particles in the relativistic region are presented. With the emphasis mainly directed to the X-ray region of the transition radiation, certain modes of application of the transition radiation for the identification and separation of relativistic charged particles are discussed. Some recent developments in detection techniques and improvements in detector performances are presented. Experiments have also been carried out to detect the "dynamic radiation", but no evidence of such an effect was observed within the sensitivity of the present experiments.

1. - INTRODUCTION

Since the early introduction of the use of transition radiation as a possible method for the detection and identification of ultra-relativistic charged particles, a number of investigations[1-7] have been made demonstrating the feasibility of such detection methods. Intensive studies[8-22] were carried out, particularly in the past few years, on the practical aspects of the detection techniques and on the application of such detection methods to high-energy cosmic-ray experiments, as well as to experiments in the high-energy accelerators, primarily for particles in the ultra-relativistic region. Results obtained thus far show great promise in the usefulness of the transition radiation detector technique for identification of particles in the range of Lorentz factor γ ($= E/m_0c^2$) between $\sim 10^3$ and $\sim 10^6$. Furthermore, it appears to be feasible, under certain conditions, to separate electrons, pions, protons, and kaons, in the energy range of a few GeV up to a few hundred GeV, in the present range of accelerator experiments.

The present paper is intended to give: in Section 2, firstly, a brief review of the important characteristics of the transition radiation both in the optical and in the X-ray region; and secondly, a summary of the major experimental achievements obtained in the past few years especially in the verification of these theoretically predicted characteristics; in Section 3, a brief description of the aspects and modes of application of transition radiation; in Section 4, a resumé of some recent results on the investigation and optimization of technical parameters in a practical transition radiation detector design; in Section 5, some general conclusions on the important advantages of such a detector; and in Section 6, some experimental results on the detection of the "dynamic radiation" emitted from a crystal lattice by the passage of a relativistic particle.

2. - A BRIEF REVIEW OF THE IMPORTANT CHARACTERISTICS OF TRANSITION RADIATION

It would be worth while to give a brief review of some of the principal characteristics in the nature of transition radiation for those who are not familiar with this subject.

When a uniformly-moving charged particle traverses from one medium, having a dielectric constant ε_1, and magnetic permeability μ_1, crossing the boundary into a second medium, having a dielectric constant ε_2, and a magnetic permeability μ_2, energy is lost by the particle at the boundary (or interface) between the two media and this energy loss is emitted in the form of electromagnetic radiation known as the transition radiation. Ginzberg and Frank[23] first predicted the existence of the transition radiation in 1946 and Garibian[24] developed the theory later for relativistic particles into a more practically applicable formulation as well as extending it into the X-ray region. For simplification, one of the media is assumed to be a vacuum ($\varepsilon_1 = 1$ and $\mu_1 = 1$). Hence the expression of the energy of the transition radiation emitted per unit solid and per unit frequency interval from an interface between vacuum and a medium of dielectric constant $\varepsilon_2 = \varepsilon$, $\mu_2 = 1$, at an angle θ from the direction of the traversing particle, is given by

$$\frac{d^2W}{d\Omega\, d\omega} = \frac{e^2}{\pi^2 c}\,\frac{\beta^2 \sin^2\theta \cos^2\theta}{(1-\beta^2\cos^2\theta)^2}\left|\frac{(\varepsilon-1)(1-\beta^2 \mp \beta\sqrt{\varepsilon-\sin^2\theta})}{(\varepsilon\cos\theta + \sqrt{\varepsilon-\sin^2\theta})(1 \mp \beta\sqrt{\varepsilon-\sin^2\theta})}\right|^2 , \qquad (1)$$

---

*) Work performed under the auspices of the U.S. Atomic Energy Commission in collaboration with the National Aeronautics and Space Administration.

**) Visitor at CERN, Geneva, Switzerland.

where the dielectric constant $\varepsilon(\omega) = 1 - [\omega_p^2/\omega(\omega + i\delta)]$ is a complex quantity, and the plasma frequency ω_p is given by the well-known expression

$$\omega_p^2 = \frac{4\pi N_e^2}{m_e} , \qquad (\hbar\omega_p)_{Al} \approx 34 \text{ eV} ,$$

and δ is related to the inverse of relaxation time which is quite small ($\hbar\delta \sim 0.2$ eV). The + sign refers to the backward emission and the - sign refers to the forward emission.

The frequency of the transition radiation extends upward with the γ of the charged particle in question. The upper limit of the emitted frequency is given by $\gamma\omega_p$. For a particle with $\gamma = 10^3$, the cut-off energy is $\sim$ 34 keV for aluminium, which is well in the X-ray region.

By integrating Eq. (1) over all angles, assuming $\beta \simeq 1$, Garibian[24] obtained the expressions for the total energy emitted by the transition radiation from a single interface both for the optical region and for the X-ray region:

$$\text{in the optical region:} \quad W_{opt} = \frac{2e^2}{c} (\ln 2\gamma - 3/2)\, \Delta\omega , \tag{2}$$

where $\Delta\omega$ is the range of optical frequencies and

$$\text{in the X-ray region:} \quad W_{X\text{-ray}} = \frac{2e^2\,\omega_p}{3c}\,\gamma . \tag{3}$$

Here we see that in the optical region, the total energy of the transition radiation is proportional to the logarithm of the Lorentz factor γ. On the other hand, the total energy of the transition radiation emitted in the X-ray region is <u>linearly</u> proportional to γ. In either the optical or the X-ray case, the energy of the transition radiation emitted from a single interface by a single relativistic charged particle is extremely small (the probability of emitting a single photon is $\sim$ 1%), so that a large number of interfaces are needed to obtain a large enough number of photons for the detection of a single particle. One convenient way to accomplish this is to employ a stack of thin material foils as radiator. Experiments carried out both in the optical region[6] and in the X-ray region[9] of the transition radiation have verified the theoretical predictions of the energy dependence (2) and (3).

The angle θ_m at which the maximum intensity of the transition radiation is emitted with reference to the direction of the traversing particle is $\sim 1/\gamma$ according to theory. This prediction has also been verified experimentally[9] in the X-ray region.

Furthermore, the energy spectra of the X-ray transition radiation for different values of γ ranging from $\gamma = 1000$ up to $\gamma = 20{,}000$ have been measured experimentally[9] and are in reasonably good agreement with theory.

As was first pointed out by Garibian[24] theory also predicts that there exists a minimum thickness of the medium (material or vacuum) that the particle must traverse before the transition radiation can be created. This minimum thickness is generally known as the formation zone Z, and is essentially the distance in which the particle field and the photon field interact coherently.

For relativistic particles, the formation zone is given by

$$z = \frac{c}{\omega} \frac{1}{(1/\gamma)^2 + \frac{1}{2}(\omega_p/\omega)^2} . \tag{4}$$

The dependence of the material (foil) formation zone and the vacuum formation zone is shown in Fig. 1. Employing a stack of thin metal or mylar foils with foil thickness a spaced at a distance d between adjacent foils, transition radiation in the X-ray region was measured by varying respectively the thickness a and the spacing d; the existence of such a formation zone in transition radiation in both material and in air has also been verified[12].

Experiments using channel glass as radiators in the optical region and loosely packed graphite granules of various sizes as radiators in the X-ray region have been carried out with no apparent advantage over the thin-foil radiators. However, plastic foam blocks which consist of tiny air cells have been used as radiators in the X-ray transition radiation region with varying degrees of success[12,14,17,20]. A more detailed series of tests will be described later in Section 4 of this paper. In general, the intensity of the X-ray transition radiation emitted from a stack of thin foils can be described reasonably well by the present theory.

Summarizing the above, the following list represents some of the major achievements in the TR (transition radiation) investigations:

i) Establishment of feasibility of measuring TR from a single charged particle both in the optical and in the X-ray region by the employment of multiple interfaces.

ii) Verification of the logarithmic dependence of the optical TR intensity on γ of the charged particle.

iii) Verification of the linear dependence of the X-ray TR intensity on γ.

iv) Verification of the $\theta_m \simeq 1/\gamma$ relation.

v) Measurement of the X-ray TR energy spectra for different γ's (in reasonably good agreement with theory).

vi) Verification of the "formation zone" effect in the X-ray TR intensity both for air and for material media.

vii) Essential elimination of the usually troublesome Landau tail of the ionization loss spectrum of a relativistic charged particle by means of a simple computer device.

viii) Verification, in general, of the intensity of TR X-rays emitted from a thin-foil stack radiator as predicted by theory.

3. - ASPECTS AND MODES OF APPLICATION OF TR

As pointed out earlier, the intensity of TR even from multiple interfaces is, in general, very low; therefore the application of TR as relativistic particle detectors requires careful studies in many respects in order to overcome some problems related to the specific modes of application. These problems remind us of the similar situation existing in the early stages of the application of Čerenkov radiation as a particle detector.

We can list two main aspects of utilizing TR for the detection and identification of relativistic charged particles. Both these aspects involve the use of the X-ray TR and are potentially very powerful methods in view of the basic characteristics of the X-ray TR stated in Section 2 above.

3.1 - Aspect I: to measure γ of an ultra-relativistic particle

If we take a proton and a pion of the same energy E, where $E = \gamma m_0 c^2$ and m_0 is the mass of the particle, then

$$\gamma_\pi/\gamma_p = m_p/m_\pi = 6.7 \ . \qquad (5)$$

Thus we see that knowing the energy of the proton and of the pion with reasonable accuracy, one does not need high accuracy in the measurements of the γ's to identify these two particles. Similarly, for kaons and pions the mass ratio $\gamma_\pi/\gamma_K = m_K/m_\pi = 3.5$ for the same energy and the mass ratio for pions and electrons $\gamma_e/\gamma_\pi = m_\pi/m_e = 280$. Under certain specific conditions, one should be able to identify these particles by measuring their γ's.

By combining[10,11] the energy distribution of the photon production process and the energy distribution of the X-ray TR we obtain the resolution in γ when measuring the total energy of the emitted TR which is given by

$$\frac{\Delta\gamma}{\gamma} \approx \sqrt{\frac{2}{n}} \ , \qquad (6)$$

where n is the number of TR photons. Therefore if one can obtain 100 TR photons, one can get a resolution in γ of $\sim$ 14%.

From the energy distribution of the TR X-rays it can be easily seen that the preponderant number of TR X-ray photons lie in the low-energy part of the energy spectrum, and that the number of photons decreases monotonously with increasing X-ray energy. Hence it would be highly advantageous to use an X-ray detector which has a high detection efficiency for low-energy X-rays.

3.2 - Aspect II: separation of particles

It could be used in such applications where one needs only to separate different kinds of particles, for example to separate π's from protons, electrons from hadrons, etc. In some cases this aspect is much easier to carry out than Aspect I. Some examples of this aspect are given in Ref. 16.

In either of the above two aspects of applications we have in practice two general modes of utilization. These are as follows:

3.3 - Small solid angle mode of utilization

In this class of utilization, where a well-defined particle beam is available such as in one of the secondary beams in an accelerator, a deflecting magnet is usually employed to deflect the particles away from the TR X-ray detector, so that the detector detects only the pure X-ray photons without the interference from any signal which would have been caused by the ionization loss of the primary particle should there be

no deflecting magnet present. Since the gain obtainable in the TR X-ray intensity by increasing the number of interfaces (e.g. the number of thin foils in a radiator stack) is limited by the simultaneous increase in absorption of the X-rays, a radiator with an optimum number of interfaces is usually chosen for a specific detector element. A cascade of several such detector elements can be easily installed in a beam transport system to increase the gain in the number of photons several fold. The number of the cascades is limited by the multiple scattering effect caused by the total amount of radiator material placed in the path of the particle. An example of the Aspect I arrangement is shown in Fig. 2a.

3.4 - Large solid angle mode of utilization

This class of utilization includes cosmic-ray experiments, high-energy experiments in space, and reaction studies in accelerator experiments, which usually require a large solid angle of investigation. In such applications it would not be possible to make convenient use of magnetic field to deflect the primary particle away from its emitted TR from a radiator. Hence the primary particle must traverse the same detector in which the TR signal is measured, and it would be necessary to subtract out from the combined signal the ionization loss dE/dx of the primary particle in the detector. Owing to the presence of the well-known high-energy "Landau" tail of the ionization loss distribution in a "thin" detector, it has always been a difficult problem to measure with certainty the ionization of a single relativistic charged particle in such a detector. As described in an earlier publication[14] by the use of a geometric-mean computing device in a detector system consisting of segmented radiator elements arranged in alternate fashion with X-ray detector elements (similar to a multi-layered sandwich), the Landau tail can be essentially eliminated. Such a detector arrangement also possesses the advantage that the low-energy X-rays would be detected by the adjacent detector before they could be absorbed in a continuous stack of radiators. Figure 2b shows such a typical sandwich detector arrangement.

3.5 - General comments

In the present state of the art, the best kind of X-ray TR detector for the Aspect I utilization is a thick solid-state detector such as the Ge(Li)-detector, which has a high efficiency for detecting high-energy X-rays of the order of a few hundred keV. On the other hand, the most practical and convenient type of X-ray detector which has a high efficiency for detecting low-energy X-rays ($\sim$ 5 to 10 keV) for the large solid angle mode of utilization seems to be the multiwire proportional chambers, although streamer chambers have also been used to great advantage[19,20]. A proposed arrangement of a possible cosmic-ray experiment using a TR detector system is shown in Fig. 3.

4. - SOME RECENT RESULTS ON THE OPTIMIZATION OF TECHNICAL PARAMETERS IN A PRACTICAL DETECTOR DESIGN

In order to design a practical TR detector, especially for the large solid angle mode of utilization, it is essential to consider not only the formation zone effect, the absorption factor, etc., but also a number of other technical parameters which should be carefully studied and well understood so that one can use this knowledge as a basis to design the optimum detector system for any specific application and within a certain desired range of particle energy or γ. These technical parameters include the radiator material, the geometry of the multiple interfaces (orderly spaced or randomly spaced), the thickness of the MWPC (multiwire proportional chamber); the gas mixture used in the MWPC, the rejection ratio of the undesired particle as a function of the number of sandwich layers, and the particle energy or γ dependence of such a detector system also as a function of the number of sandwich layers, etc.

The following is a resumé of the results of the recent investigations on optimizing the technical parameters in a practical detector design obtained by the Brookhaven group which consists of H. Uto, G.F. Dell, A. Bamberger, P.W. Alley and the author. These investigations were carried out at the Brookhaven 32 GeV AGS test beam with the primary objective of optimizing the technical parameters in a sandwich-type detector system for both large solid angle and small solid angle modes of application. This detector system consists of alternate layers of radiator segments and MWPC similar to that shown in Fig. 2b.

Because of limited space the details of the results of these investigations will not be presented here, but will be published elsewhere.

4.1 - Radiator material

Plastic foam material with different sizes of air bubbles but having essentially the same density was studied to compare their respective efficiencies in producing TR. Some of the smaller bubble sizes in the plastic foam were obtained by compressing a normal foam block down to ¼ of its original thickness. The results obtained show that the foam material having the largest bubble size available, namely ½ mm in size, is the most effective radiator in the X-ray region. However, a radiator stack of 100 mylar foils each 0.5 mil thick with 60 mil spacing between two adjacent foils, gives a 40% higher yield of TR X-rays than a 4 in. thick foam for particles of $\gamma = 2.7 \times 10^3$. Furthermore, plastic foam with irregular sizes of bubbles yields less TR intensity than that with uniform size bubbles.

In Fig. 4 the black dots show the relative TR signal in four argon-filled MWPC each 2.2 cm thick as a function of foil thickness in four segmented radiator stacks (each containing 50 mylar foils) at an electron energy of 2.7 GeV. The circles are the corresponding values calculated from theory. The left-hand part of the curve shows an increase in signal with foil thickness which is attributable to the formation zone effect. The right-hand part shows a decrease in signal with foil thickness which is due to the increasing overriding absorption of the thicker foils. 0.5 mil thick mylar foils seem to give the best TR signal. The agreement between the measured values and the theoretically predicted values is quite good.

The dependence of the TR signal on the foil spacing is shown in Fig. 5. It is similar to the detector system employed in the case of Fig. 4, with the exception that the mylar foil thickness is fixed at 0.5 mil and that the spacing between foils is varied between 15 and 120 mil. The black dots indicate the experimental results, whereas the solid line represents the theoretically expected values based on the multifoil formula. The agreement between theory and experiment is reasonably satisfactory. It appears that a spacing of > 30 mil would be optimum in this energy region.

4.2 - Effect of the thickness of the MWPC and gas mixture

When we measure the TR intensity in a combined signal of TR and particle ionization loss, it is apparent that the thickness of the MWPC and its gas mixture must be chosen to give the maximum TR signal relative to the signal due to the particle ionization loss. Figure 6 shows the relative TR signal as a function of chamber thickness obtained with a single MWPC using argon and xenon gas respectively, and 100 foils of 0.5 mil mylar at 60 mil spacing for 2 GeV electrons ($\gamma = 4000$). For the 1.2 cm chamber, the gain in the TR signal is a factor of 2 greater in using xenon instead of argon, whereas for the 2.2 cm chamber the gain is much less, indicating that the TR consists mostly of soft X-rays and consequently is absorbed in the front part of the chamber.

Figure 7 shows the relative full width at half maximum (FWHM) of the ionization loss spectrum for π's and electrons at 2 GeV/c momentum for different chamber thicknesses and gases. The abscissa is approximately proportional to the thickness of the chamber. The upper dashed curve represents the measured values without any correction for intrinsic chamber resolution. The lower dashed line represents the results of West[25], which are generally lower than the present measurements.

Figure 8 shows the mass absorption coefficients for argon, krypton, and xenon, all corrected for escaping fluorescent radiation. In the energy region of between 5 and 15 keV, where most of our interest lies in the detection of TR X-rays with a MWPC, xenon appears to be the most efficient absorber per unit of ionization loss.

The ratio of the most probable energy losses of electrons and of pions is shown in Fig. 9 for different chamber thicknesses and gases at the same momenta (2.3 GeV/c). The arrows indicate the expected values as calculated from the theoretical density effect. The most probable energy loss of electrons in all three different gases and in various thicknesses of the MWPC is always greater than the corresponding most probable energy loss of pions.

A comparison of the combined signal of TR and ionization loss in using xenon as against argon in a 4-MWPC thin chamber (1.2 cm) configuration for 2.7 GeV/c electrons ($\gamma = 5400$) is shown in Fig. 10, where the probability distribution is plotted for photon absorption as a function of the total geometric mean energy of the TR. It is seen that even with as few as a 4-chamber configuration the advantage of using xenon in a thin chamber is quite apparent. For comparison, a similar distribution for a single thin xenon chamber is shown in Fig. 11, where the probability of photon absorption is $\sim$ 40% and the relative shift of the averages due to TR is 44%.

Some preliminary results on the use of a mixture of three gases, namely xenon, methane and helium have shown extremely encouraging indications that the ratio of the TR signal to the particle ionization loss can be vastly improved. Figure 12 shows that in a thin chamber (1.2 cm) for a counter gas mixture of 34% Xe, 9% CH_4, 57% He, the ratio of the 6 keV signal (mean TR signal in a MWPC) to the β ionization loss signal increases by a factor of 2 over that in a normal argon-methane mixture.

4.3 - Energy dependence and general performance of multichamber TR detection systems

The energy dependence characteristics of a 10-chamber sandwich-type TR detection system have been studied using normal argon-filled chambers with two different kinds of radiator segments. In Fig. 13 the black dots are the measurements obtained with 4 in. thick styrofoam blocks as radiator segments, whereas the circles represent those obtained with stacks of 100 mylar foils of 0.5 mil thickness and a spacing of 60 mil as radiators. The yield Y is the relative energy deposit of TR in terms of the average energy loss for background radiators. The solid line represents the theoretical calculation for the stacks of mylar foils. The absolute scale has an over-all error of $\sim$ 15%. It is apparent that the mylar foil radiators are appreciably better than the foam radiators of comparable dimensions, and that the energy dependence in such a detector system is fairly linear within the energy range investigated.

Figure 14 shows the pulse-height distribution due to TR and ionization loss for a 10-chamber detection system using 4 in. styrofoam blocks as radiator segments for electrons and pions of 2.7 GeV/c. Fig. 14a

represents the measurements obtained using the arithmetic mean, while Fig. 14b represents the values obtained employing the geometric mean computer device. The dashed lines in Fig. 14b represent the expected result for a 30-chamber detector system based on the measured values. Even with the argon-filled chambers and the less efficient foam radiators, the separation between electrons and pions at 2.7 GeV/c can be easily achieved.

Measurements obtained with a similarly arranged 20-chamber detector system are shown in Fig. 15. The pion distribution remains the same with or without the radiators, since the γ of the pions is too small ($\gamma_\pi \simeq 50$) to yield any detectable TR.

Using the measurements shown in Fig. 15 we can calculate the pion contamination of the signal for the 20-chamber (argon-filled) detector system with foam radiators for equal numbers of electrons and pions present. This contamination occurs when the pion-induced signal exceeds a discriminator level set to include the desired fraction of electrons. In Table 1 the pion contamination is calculated for 50% and 90%, as the desired fraction of electrons. The following conclusions can be drawn from these calculations:

i) Mylar foils are a factor of 2 more efficient than foam radiators in this particular 20-chamber system.

ii) Using 20 chambers instead of 10 gives an improvement of a factor of 2-3.

iii) Using twice as many chambers, but keeping the over-all length of the radiator constant, gives an improvement of a factor of 2.

iv) The geometric mean saves a factor of 2 in the number of chambers as opposed to the arithmetic mean.

It should be pointed out that these conclusions are based only on the argon-filled chambers of medium thickness, whereas much improvement can be expected if Xe-CH_4-He-filled thin chambers are used. Furthermore, the performance of the geometric mean computer device for the 20-chamber system may be improved to eliminate the Landau tail more effectively as it is supposed to do.

Table 1

Pion contamination in percentage

Radiator	50% accepted electrons				90% accepted electrons			
	10 chambers		20 chambers		10 chambers		20 chambers	
	Arith. mean	Geom. mean	Arith. mean	Geom. mean	Arith. mean	Geom. mean	Arith. mean	Geom. mean
4 in. foam	5.0	0.8	1.6	0.29	20.0	7.6	11.0	2.0
100/0.5/60	3.2	0.34	-	-	13.8	4.7	-	-
2 in. foam	-	-	2.65	0.38	-	-	15.6	2.54
50/0.5/30	-	-	1.22	0.25	-	-	8.6	1.4

5. - GENERAL CONCLUSIONS ON THE IMPORTANT ADVANTAGES OF A TR DETECTOR USING THE X-RAY PART OF THE SPECTRUM

i) It can measure γ of a charged particle instead of measuring β.

ii) It can separate different kinds of relativistic particles within certain limitations.

iii) It has a linear energy-dependence characteristic.

iv) It gives uniquely the direction of the measured particle.

v) It presents very low mass in the path of the primary particle.

6. - DETECTION OF "DYNAMIC RADIATION"

In an attempt to verify the "dynamic radiation" first predicted theoretically by Garibian[26] and later observed experimentally by Alikhanian et al.[27,28] we have set up an experiment at the Brookhaven AGS test beam using thin crystal plates of mica. We have employed both a MWPC and a NaI counter as the X-ray detector. We have also used plastic foam and mylar foils as radiators for TR for comparison.

Figure 16 shows the results of the study of "dynamic radiation" with a MWPC, 2.2 cm thick filled with argon. The circles represent measurements of the signal obtained from four sheets of mica each of which is 15 mil thick traversed by electrons of 7 GeV energy (γ = 14,000). The solid line represents the transition radiation obtained from a 4 in. thick plastic foam and the dashed line represents the background signal due to a solid polystyrene sheet, 0.1 in. thick. It appears that the radiation from the mica sheets is close to the background radiation, giving no evidence of the "dynamic radiation".

Figure 17 shows the results of a similar investigation using a NaI counter (2 in. in diameter and ½ in. thick). The circles represent the measured radiation from a 24 mil thick mica sheet by electrons at 2.7 GeV/c. The solid line represents the TR signal from a mylar stack radiator (230 foils of 1 mil thickness with 32 mil spacing). The dashed line represents the background radiation from a 0.1 in. polystyrene sheet. It seems that no "dynamic radiation" is evident from a 24 mil thick mica sheet.

Further investigations on the "dynamic radiation" are in progress.

References

1) P. Goldsmith and J.V. Jelley, Phil. Mag. 4, 836 (1959).

2) A.I. Alikhanian, Loeb Lectures, Harvard University, February 1965 (unpublished).

3) A.I. Alikhanian, Lecture notes, Fifth Session of the Spring School of Experimental and Theoretical Physics, Armenian Academy of Sciences, Yerevan, USSR, 1965 (unpublished), p. 651.

4) F.R. Harutyunian, K.A. Ispirian, A.G. Oganessian, Yadernaya Fiz. 1, 842 (1965).

5) F.W. Inman and J.J. Muray, Phys. Rev. 142, 272 (1966).

6) J. Oostens, S. Prünster, C.L. Wang and L.C.L. Yuan, Phys. Rev. Letters 19, 541 (1967).

7) S. Prünster, C.L. Wang, L.C.L. Yuan and J. Oostens, Phys. Letters 28 B, 47 (1968).

8) L.C.L. Yuan, C.L. Wang and S. Prünster, Phys. Rev. Letters 23, 496 (1969).

9) L.C.L. Yuan, C.L. Wang, H. Uto and S. Prünster, Phys. Letters 31 B, 603 (1970).

10) L.C.L. Yuan, C.L. Wang, H. Uto and S. Prünster, Phys. Rev. Letters 25, 1513 (1970).

11) L.C.L. Yuan, Proc. 11th Int. Conf. on Cosmic Rays, Budapest, 1969 (Akadémiai Kiado, Budapest, 1970), Vol. 4, p. 553.

12) L.C.L. Yuan, Proc. 12th Int. Conf. on Cosmic Rays, Hobart, Tasmania, Australia, 1971 (Hobart, 1971), Vol. 4, p. 1499.

13) L.C.L. Yuan, *in* Proc. 12th Scintillation and Semiconductor Counter Symposium, Washington, D.C., 1970, IEEE Trans. Nuclear Sci. NS17, No. 3, 24 (1970).

14) H. Uto, L.C.L. Yuan, G.F. Dell and C.L. Wang, Nuclear Instrum. Methods 97, 389 (1971).

15) L.C.L. Yuan, H. Uto, G.F. Dell and P.W. Alley, Phys. Letters 40 B, 689 (1972).

16) C.L. Wang, G.F. Dell, H. Uto and L.C.L. Yuan, Phys. Rev. Letters 29, 814 (1972).

17) A. Lamberger, G.F. Dell, H. Uto, L.C.L. Yuan and P.W. Alley, Phys. Letters 43 B, 153 (1973).

18) A.I. Alikhanian et al., JETP Letters 11, 347 (1970).

19) A.I. Alikhanian, K.M. Arakian, G.M. Garibian, M.P. Lorikian, K.K. Shikhilarov, Phys. Rev. Letters 25, 635 (1970).

20) A.I. Alikhanian, G.M. Garibian, M.P. Lorikian and K.K. Shikhilarov, JETP Letters 16, 201 (1971).

21) A.I. Alikhanian, E.S. Belyakov, G.M. Garibian, M.P. Lorikian, K.Zh. Markarian and K.K. Shikhilarov, JETP Letters 16, 315 (1972).

22) F. Harris, T. Katsura, S.I. Parker, V. Peterson, R. Ellsworth, G. Yodh, W. Allison, C. Brooks, J. Cobb and J. Mulvey, Nuclear Instrum. Methods 107, 413 (1973).

23) V.L. Ginzburg and I.M. Frank, Zh. Eksper. Teor. Fiz. 26, 15 (1946).

24) G.M. Garibian, Zh. Eksper. Teor. Fiz. 37, 527 (1959).

25) G.M. Garibian, Soviet Phys. JETP 33, 1403 (1957).

26) D. West, Proc. Phys. Soc. A 66, 306 (1953).

27) A.I. Alikhanian, *in* Proc. Int. Conf. on Instrumentation for High-Energy Physics, Dubna, 1970 (JINR, Dubna, 1971), Vol. 1, p. 491.

28) A.I. Alikhanian, G.M. Garibian, M.P. Lorikian and K.K. Shikhilarov, *in* Proc. Int. Conf. on Instrumentation for High-Energy Physics, Dubna, 1970 (JINR, Dubna, 1971), Vol. 1, p. 509; and JTTP Letters 13, 142 (1971).

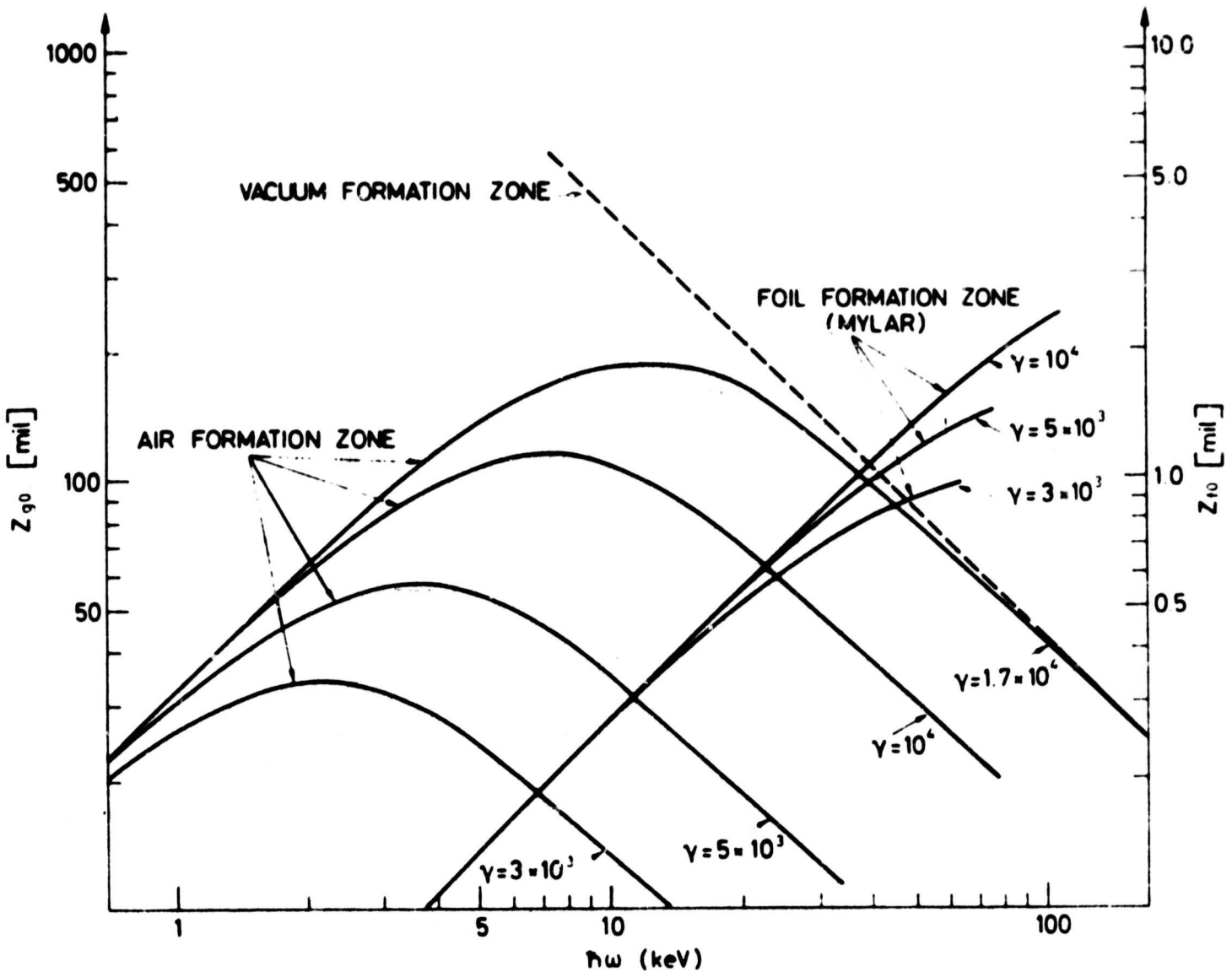

Fig. 1

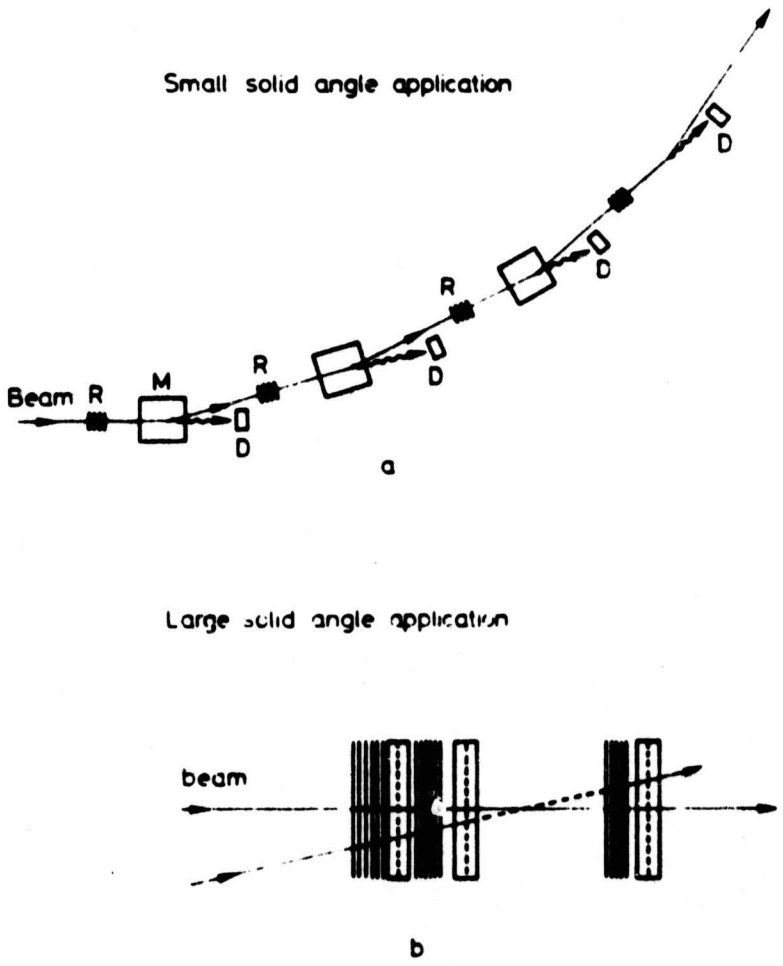

Fig. 2

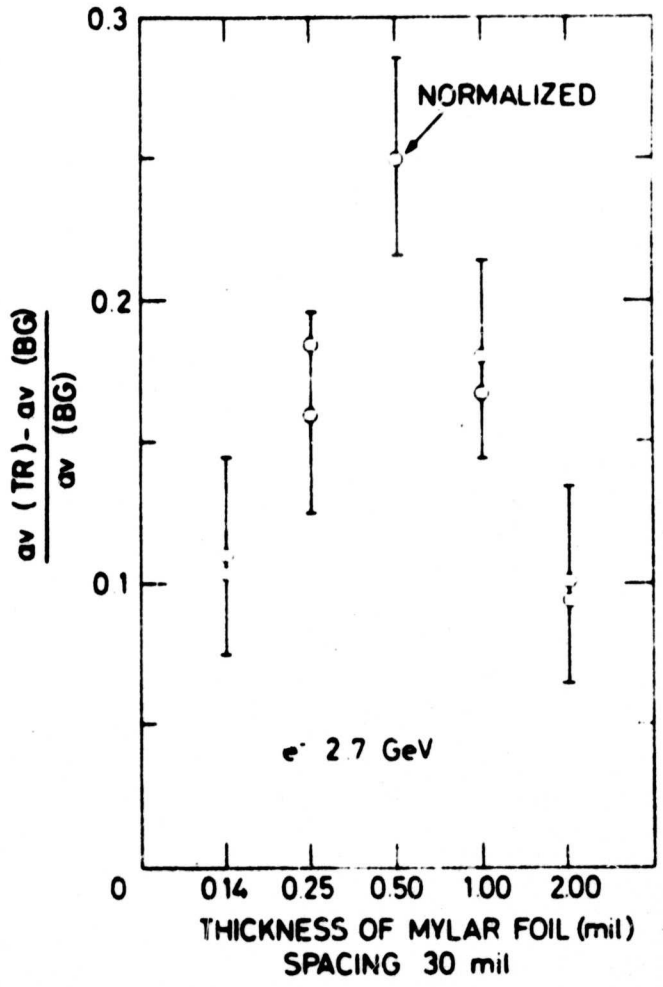

Fig. 3

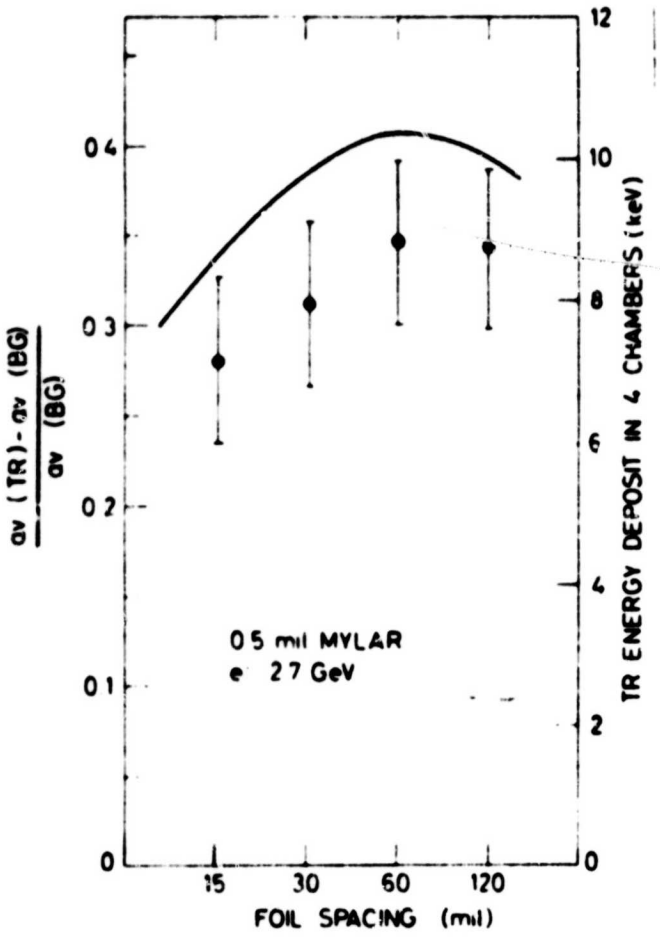

Fig. 4

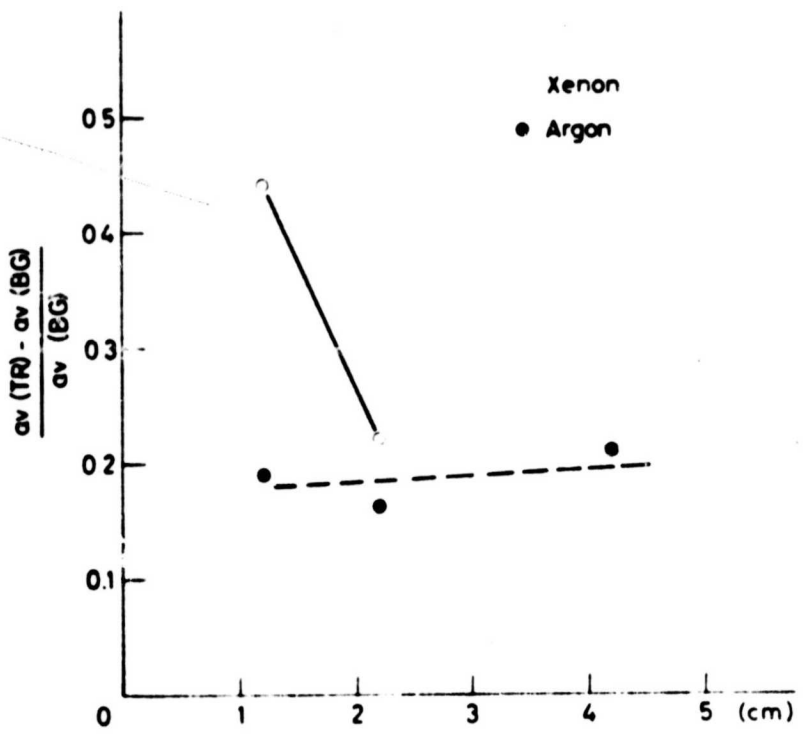

Fig. 5

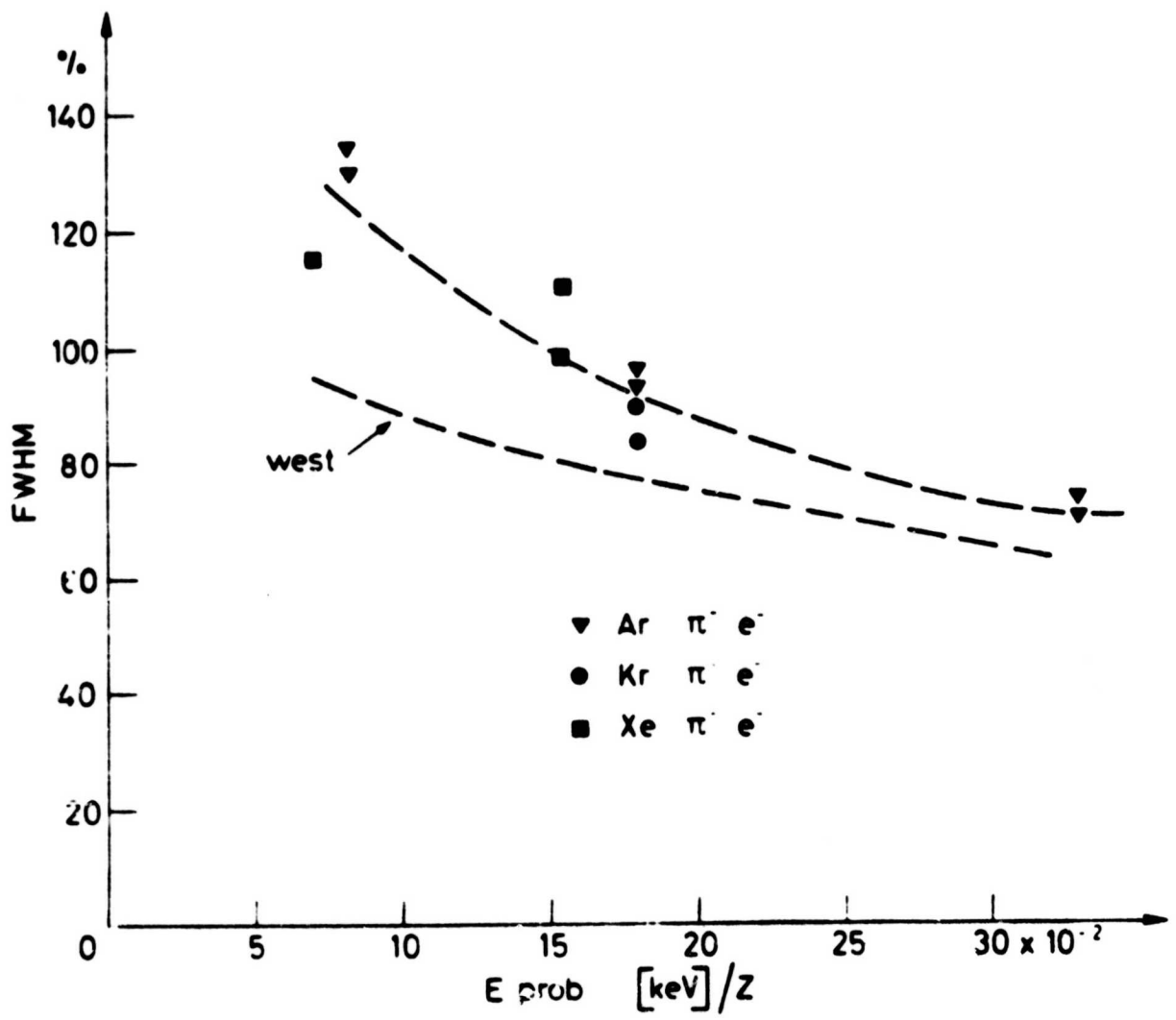

Fig. 6

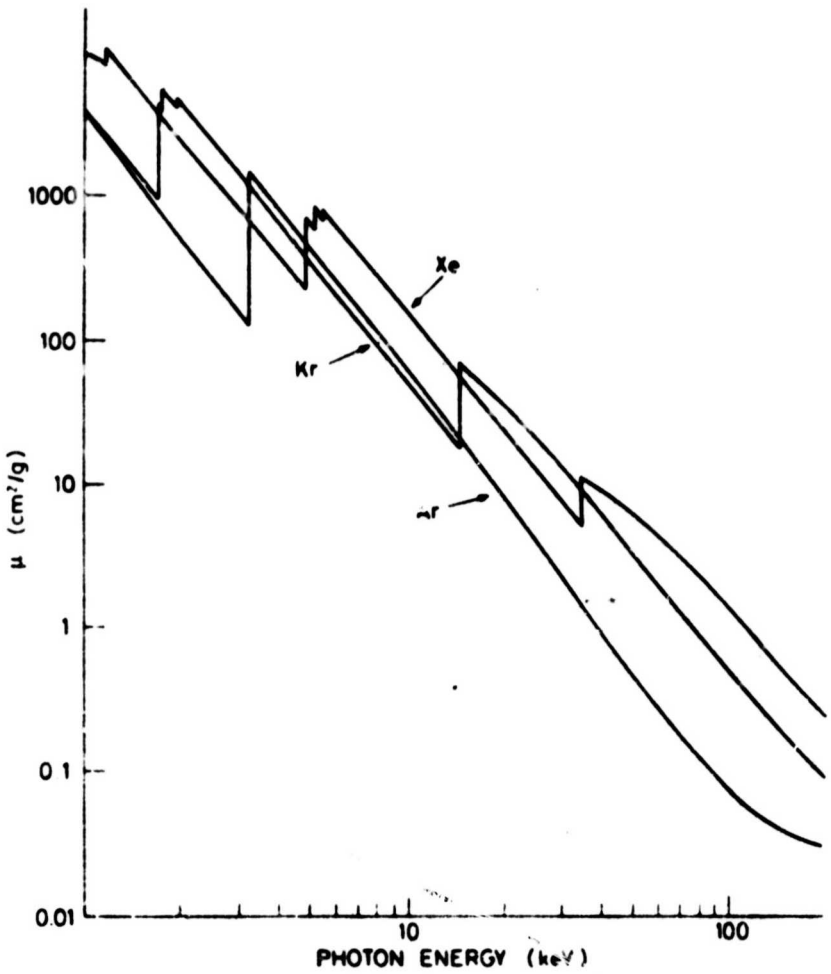

Fig. 7

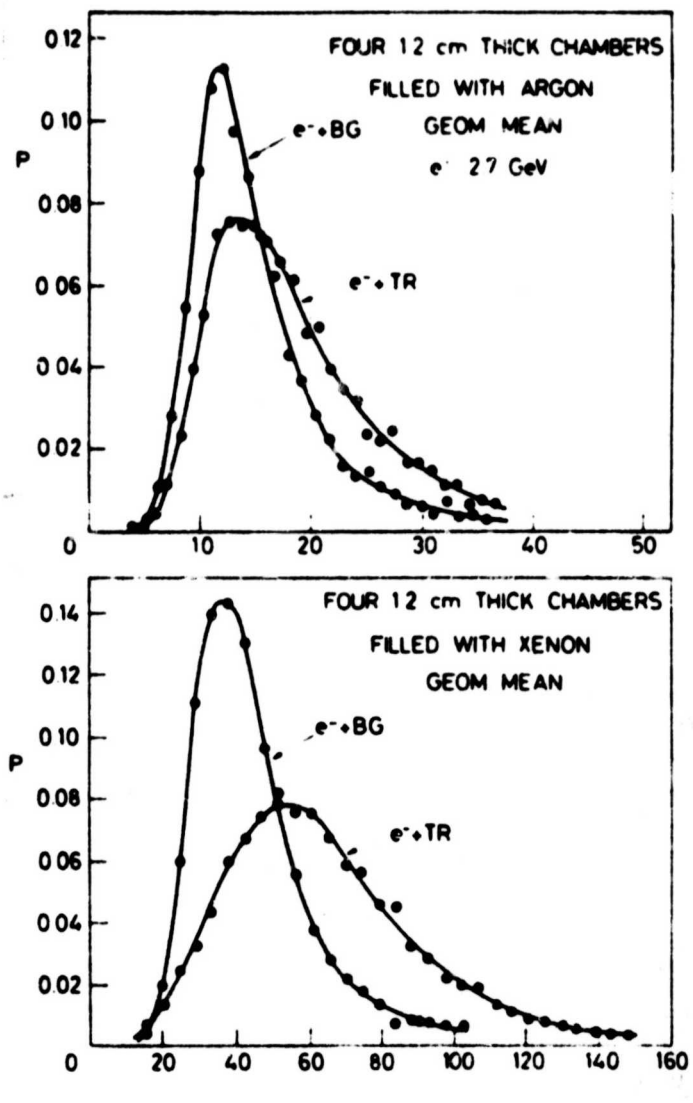

Fig. 9

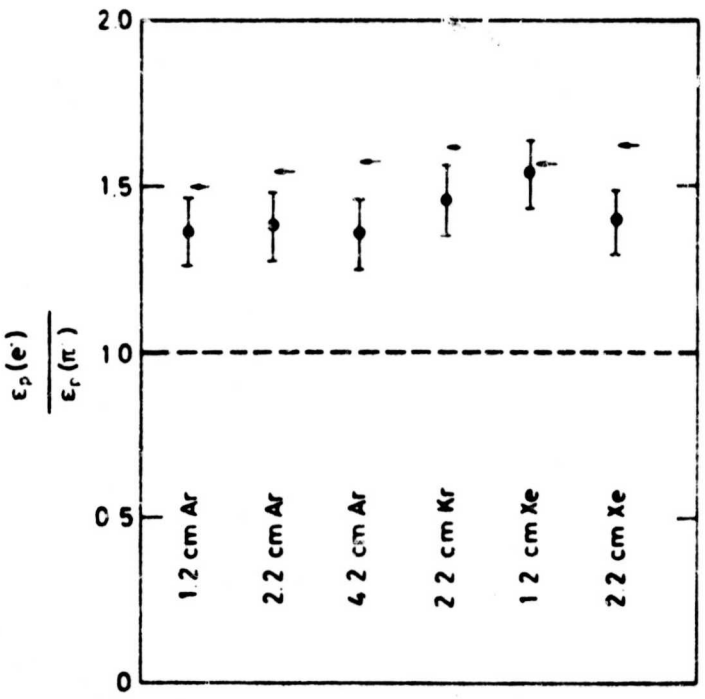

Fig. 8

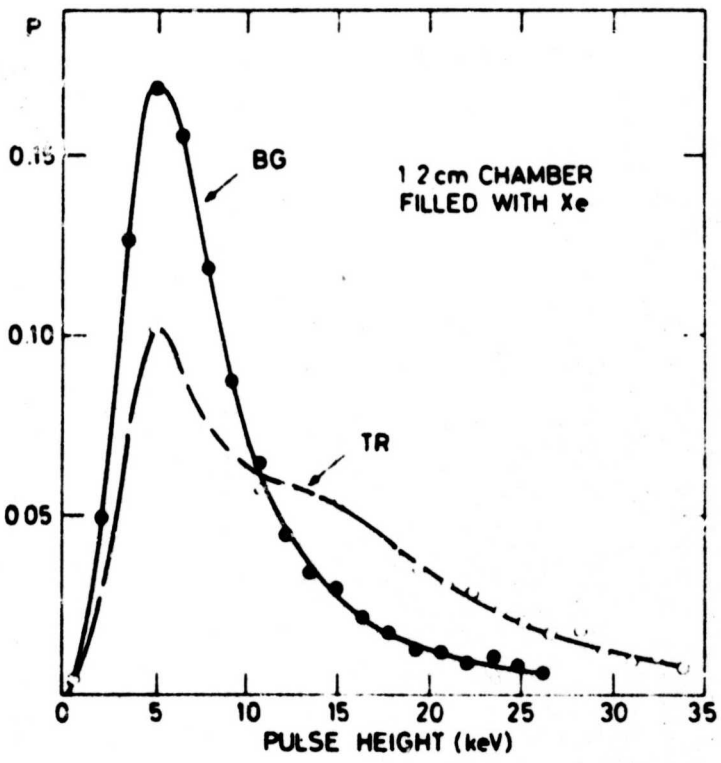

Fig. 10

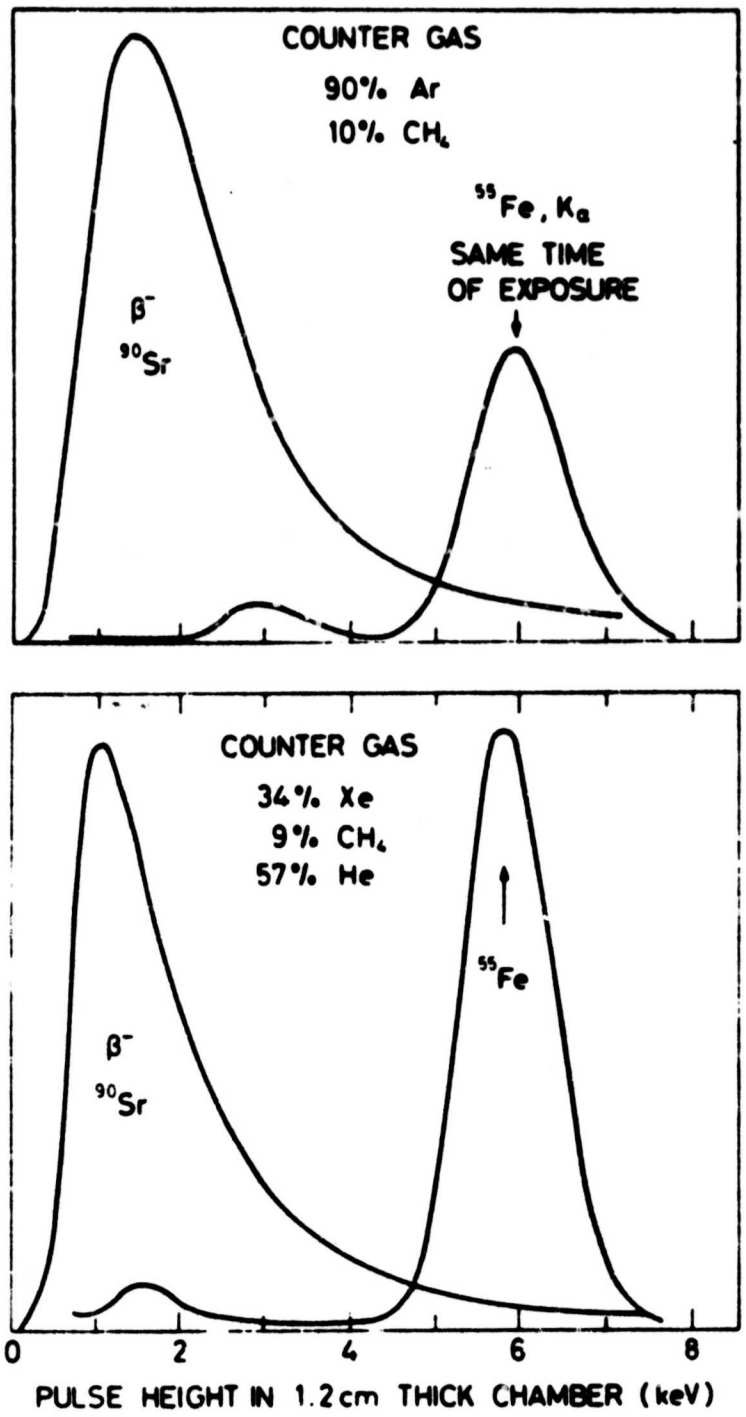
COUNTER GAS
90% Ar
10% CH4
55Fe, Kα
SAME TIME
OF EXPOSURE
β⁻
90Sr
COUNTER GAS
34% Xe
9% CH4
57% He
55Fe
β⁻
90Sr
0
2
4
6
8
PULSE HEIGHT IN 1.2cm THICK CHAMBER (keV)

Fig. 11

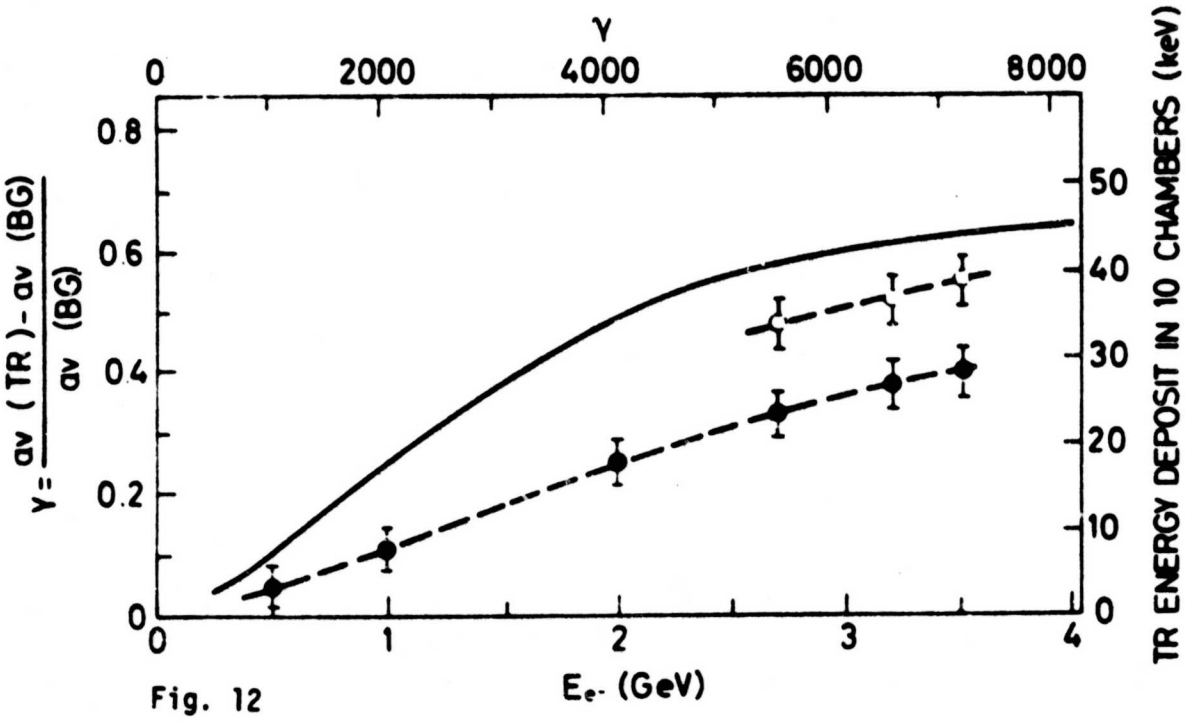
γ
0
2000
4000
6000
8000
0.8
0.6
0.4
0.2
0
50
40
30
20
10
0
1
2
3
4
Y = av (TR) - av (BG) / av (BG)
Ee- (GeV)
TR ENERGY DEPOSIT IN 10 CHAMBERS (keV)

Fig. 12

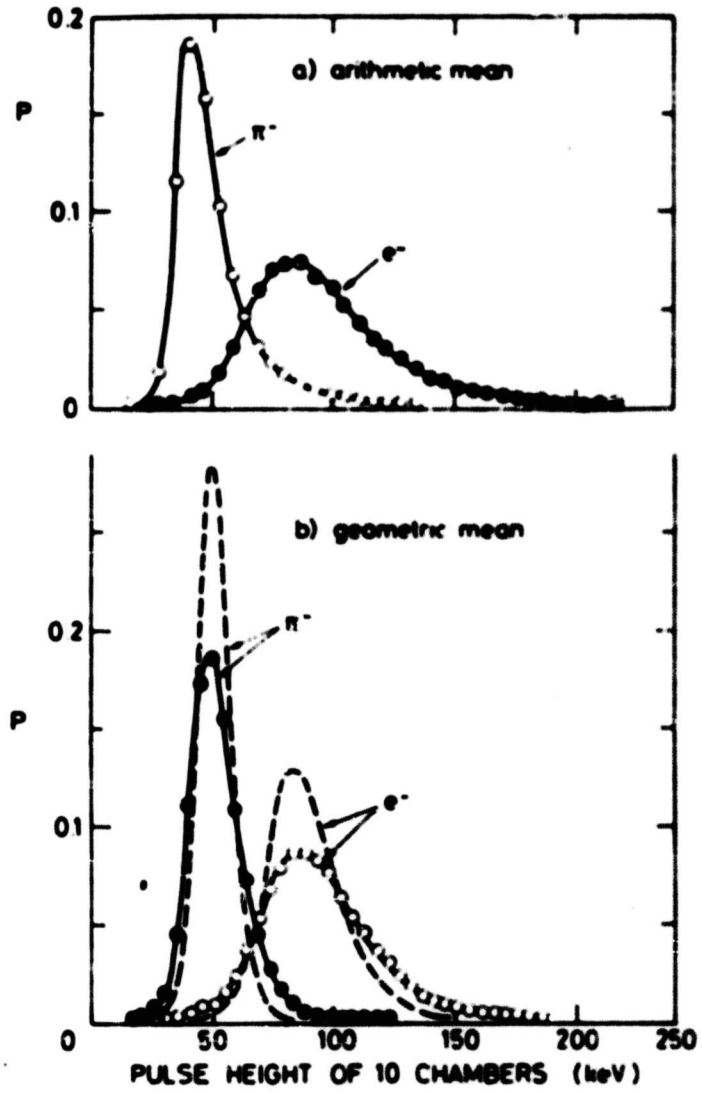

Fig. 13

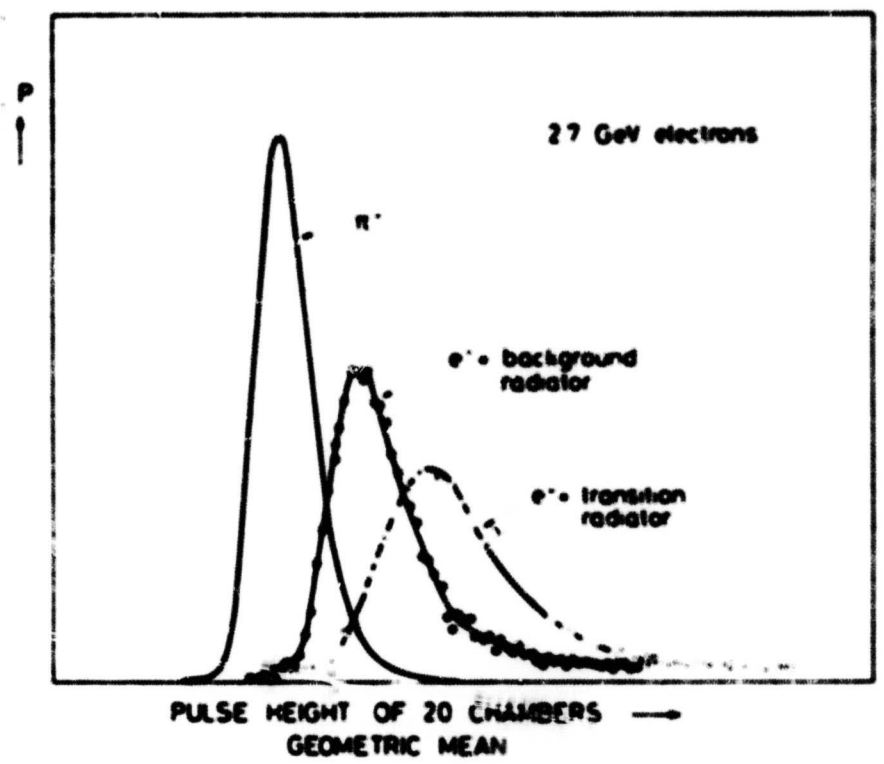

Fig. 14

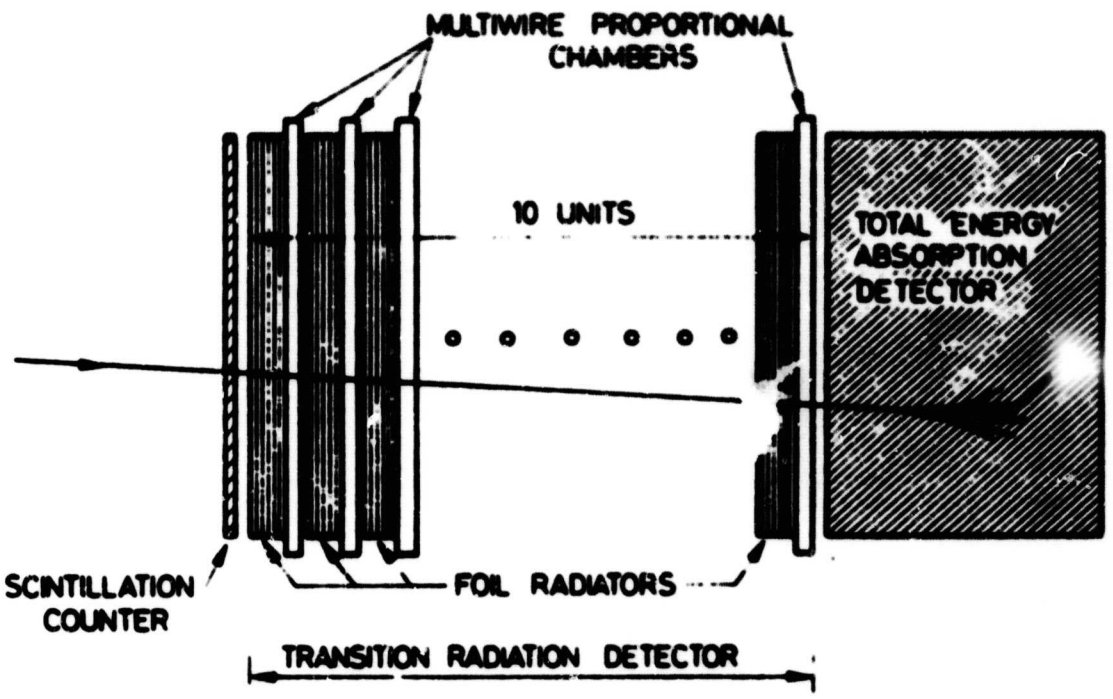

LAY-OUT FOR A POSSIBLE COSMIC RAY EXPERIMENT USING A TRANSITION RADIATION DETECTOR

Fig. 15

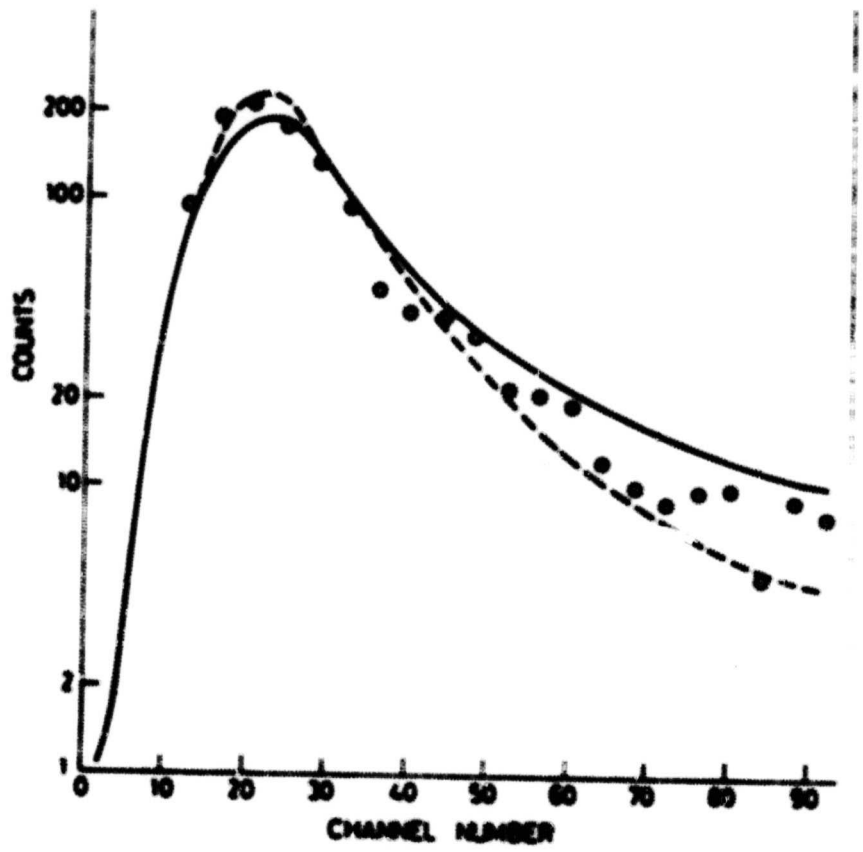
200
100
20
10
2
1
COUNTS
0
10
20
30
40
50
60
70
80
90
CHANNEL NUMBER

Fig. 16

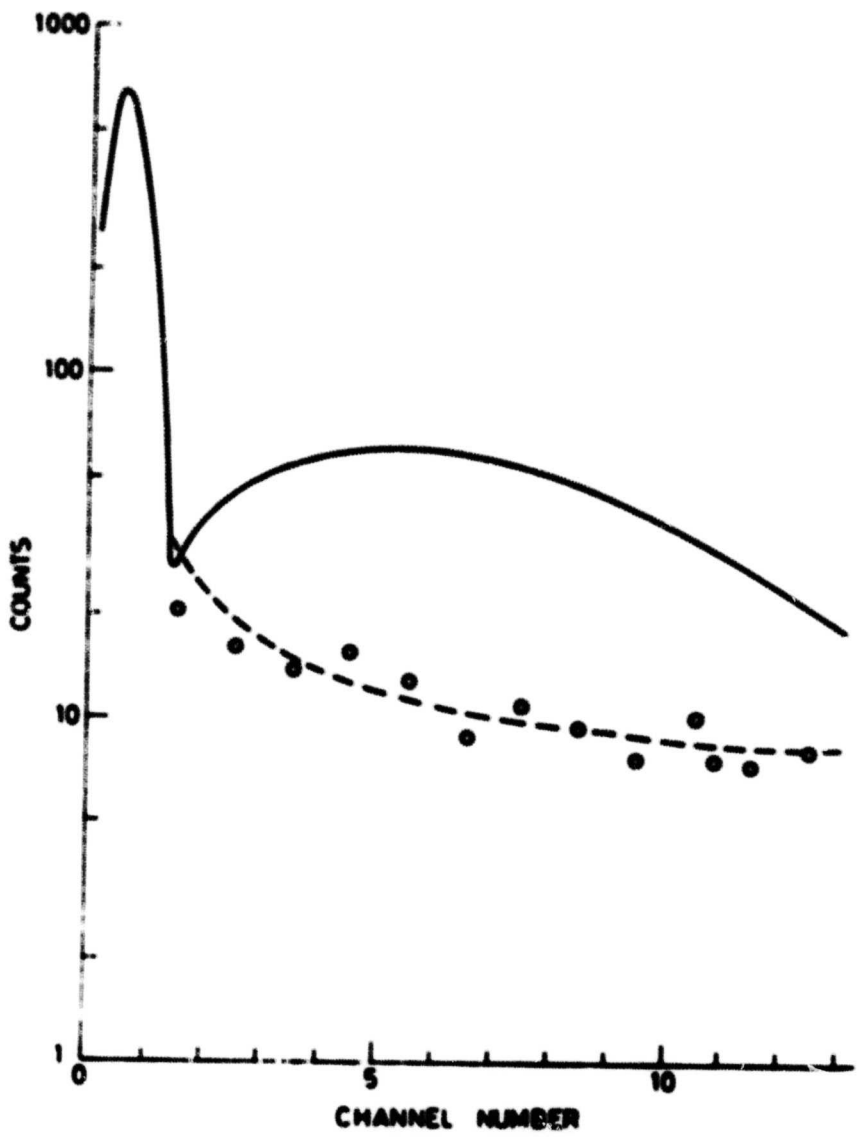
1000
100
10
1
COUNTS
0
5
10
CHANNEL NUMBER

Fig. 17